Behaviour of contact and noncontact lap compression splices

Comportamento de emenda por traspasse de barras comprimidas em contato e separadas

C. B. QUINTANA [a]
consuebello@yahoo.com.br

G. B. GUIMARÃES [b]
giuseppe@civ.puc-rio.br

L. D. SHEHATA [c]
lidiashehata@vm.uff.br

Abstract

An experimental study on the behaviour of lap splices in concrete columns under uniaxial compression is summarized herein. The objective of the study was to investigate the influence of the distance between the spliced bars on the behaviour of the lap splice. The study included tests of two columns with spliced longitudinal bars under uniaxial compression: one column with bars in contact with each other in the splice and the other with bars spaced at twice the longitudinal bar diameter φ_l. In the tested columns, it was observed that the distance between the spliced bars has an insignificant influence on the mean bond stress in the splice. At ultimate load, in both columns, the normal stress at the tip of the bars was much higher than the uniaxial concrete compressive strength.

Keywords: reinforced concrete columns, bond stress, space between spliced bars.

Resumo

Neste trabalho é resumido um estudo experimental sobre o comportamento de emendas por traspasse de barras comprimidas em pilares de concreto armado, com o objetivo de investigar a influência da distância entre as barras emendadas sobre o comportamento da emenda. O estudo englobou os ensaios à compressão centrada de dois pilares: um com emenda com barras em contato e outro com emenda com barras separadas a uma distância igual a duas vezes o diâmetro das barras da armadura longitudinal, φ_l. Nos pilares ensaiados, constatou-se que a tensão média de aderência na emenda praticamente não depende da distância entre as barras. Para ambos os pilares, próximo à carga última, a tensão normal nas pontas das barras apresentou valores muito superiores à resistência uniaxial à compressão do concreto.

Palavras-Chave: pilares de concreto armado, tensão de aderência, separação das barras emendadas.

[a] *Lecturer, Basic Industrial Course, Centro Universitário da Zona Oeste – UEZO. RJ. email: consuebello@yahoo.com.br*
[b] *Associate professor, Civil Engineering Department, Pontifícia Universidade Católica do Rio de Janeiro, PUC-Rio. email: giuseppe@civ.puc-rio.br*
[c] *Professor, Civil Engineering Department, Universidade Federal Fluminense, UFF. email: lidiashehata@vm.uff.br*

1. Introduction

The force of one bar is transferred to the other, in a lap splice, through the surrounding concrete. These forces are transferred along the splice from one bar to the concrete through bonding. In the concrete, these forces may generate elevated tangential stresses as well as radial stresses that cause the cracking of the concrete along the splice. The integrity of a splice depends on the development of an adequate bond along the surface of the bars and the capability of the concrete that involves them to transfer the tangential stresses.

Some experimental studies have been carried out to investigate the behaviour of lap tension splices, with contact and noncontact bars, in slabs (HAMAD and MANSOUR, 1996), in beams subjected to flexure (WALKER, 1951; CHAMBELIN, 1952; CHINN, FERGUSON and THOMPSON, 1955) and in pull-out tests in prisms (WALKER, 1951; CHAMBELIN, 1952). The results related to the influence of spacing of spliced bars on the bonding found in literature are, as yet, inconclusive.

Most of the research on lap splices has been done on tension splices. Compared to compression splices, the tension ones are more critical, as the concrete along the length of the splice is cracked. In general, design recommendations for compression splices have been set based on the results of tested tension splices. However, as there is greater concrete integrity in compression splices (absence of cracks), as a result of the longitudinal compression of the element, and a large part of the compression force is transferred through the tip (the study made by Pfister and Mattock, 1963, detected stresses at the tip of the bars equal to $5f_c$), there might be differences between the behaviour of the two types of splices.

The present work summarizes a part of the research carried out by Quintana (2005) on the behaviour of the bonding in a splice with contact bars and with noncontact bars ($2\varphi_l$ spacing) in rectangular cross-section reinforced concrete columns under concentric compression.

2. Experimental Programme

The experimental programme consisted of tests on two short columns under concentric compression. The variable adopted was the spacing between the lapped bars.

The columns had a 210 mm x 120 mm rectangular cross-section and a length of 1.2 m. The longitudinal reinforcement consisted of four deformed bars with nominal diameter of 16 mm. The splice length was 600 mm. The longitudinal reinforcement ratio in the region of the splice was 6.4%. Five millimetre stirrups were used.

Stirrups spaced at 20 mm were placed at the ends of the columns (last 140 mm), in order to have a greater concrete confinement and avoid failure in these regions. At the ends of the splices, the stirrups had spacing smaller than that used in the rest of the splice due to the stress concentration in these regions.

The nomenclature adopted for the columns was: PEBU and PEBS, where PE means column with splice, BU means column with contact bars in the region of the splice and BS column with bars spaced at twice the longitudinal bar diameter in the splice.

Table 1 – Concrete compressive strength		
Standard cylinders	f_c (MPa)	f_{cm} (MPa)
C-1	31,2	–
C-2	31,4	–
C-3	31,0	31,3
C-4	31,6	–

2.1 Materials and specimens casting

In order to obtain the stress-strain curve of the longitudinal reinforcement bars and the compressive strength of the concrete, specimens of these materials were tested. Figure 1 shows an example of the stress-strain curves obtained for the bars of the longitudinal reinforcement. The values of compressive strength of the cylindrical concrete specimens on the day of the test of the columns and their mean value are given in Table 1.

Figure 1 – Stress-strain diagram of longitudinal reinforcing bars

f_y = 538 MPa

E_s = 207 GPa

ε_{sy} = 0,0026
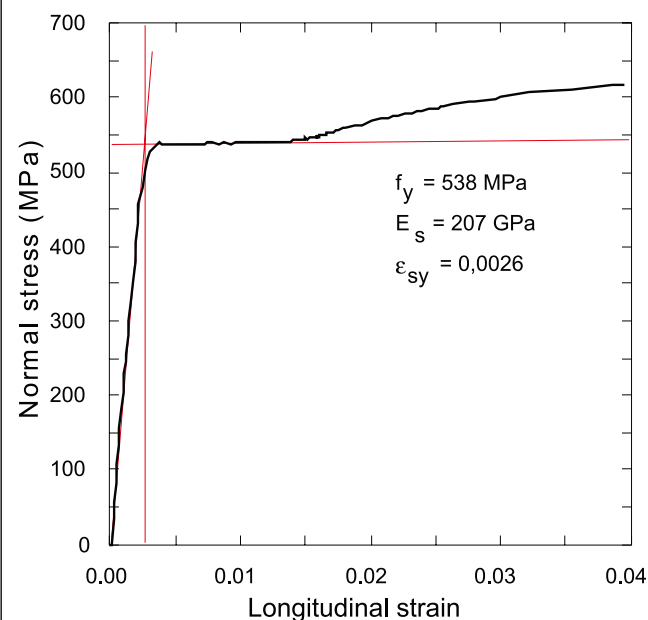
The columns were cast horizontally in wooden moulds. The concrete was compacted with the aid of a poker vibrator and cured with successive wettings for two days. The concrete had aggregate maximum size of 19 mm, 0.55 water-cement ratio, and a slump of 100 mm.

Table 2 – Columns characteristics									
Column	Cross-section (mm)	Length (mm)	Long. reinf.	Lapped bars spacing* (mm)	f_y (MPa)	ρ_l* (%)	ε_{sy} (‰)	Transv. reinf.	f_c (MPa)
PEBU	210x120	1200	$4\phi_l 16$ mm	0	544	6,4	2,7	ϕ 5 mm variable spacing	31,3
PEBS				32					

* in the splice

Figure 2 – Lateral view and cross-section of the columns (dimensions in mm)
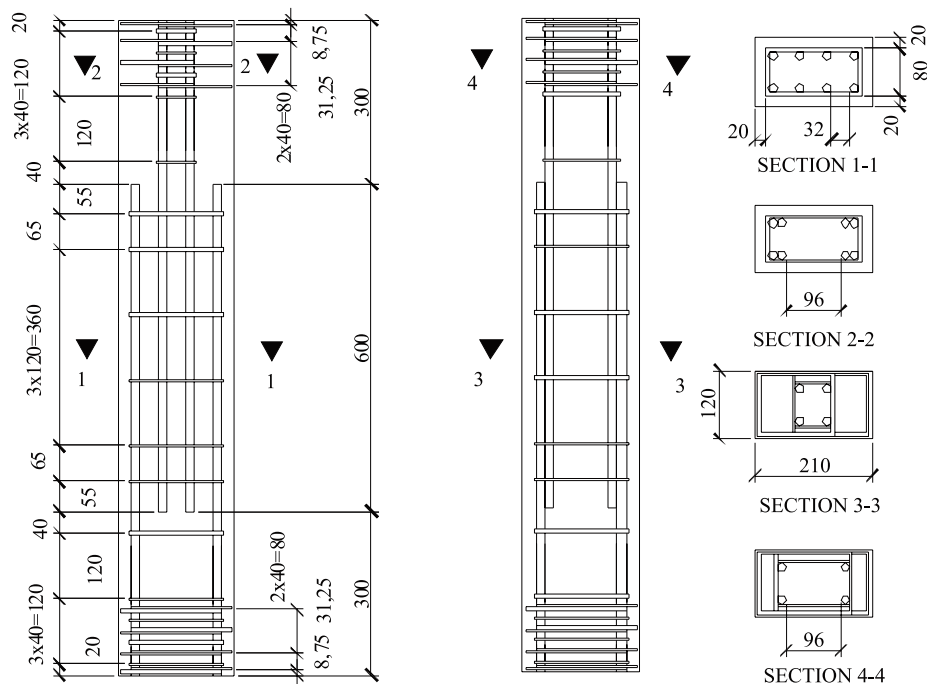
2.2 Column characteristics

Column characteristics are shown in Table 2 and in Figures 2 and 3.

2.3 Test instrumentation and procedure

Electrical resistance strain gauges with 10 mm length were used on four bars of the longitudinal reinforcement, in the region of the splices of the two columns. These bars were close to the corners diagonally opposite of the columns, as shown in Figure 4a. In both columns, some bars had three strain gauges and others five, as shown in Figure 4b.
The concrete strains in the section at midheight of the column were measured with 6.7 cm electrical strain gauges on opposite faces (Figure 5).
Steel plates were used at the bottom and top of the column and between them and the column a 10 mm thick compressible material was placed, to accommodate any irregularity, as shown in Figure 6. To fix the top of the column, a metallic device was placed around it, as shown in Figure 6a. This device was attached to the reaction frame through threaded bars, ensuring the positioning of the column. The system was designed so to allow the axial displacement of the top of the column during the test. The adjustment of the exact position of the column was easily done with the aid of the bolts that connected the support to the columns and to the frame.

Figure 3 – Columns reinforcement

(a) Column PEBS   (b) Column PEBU
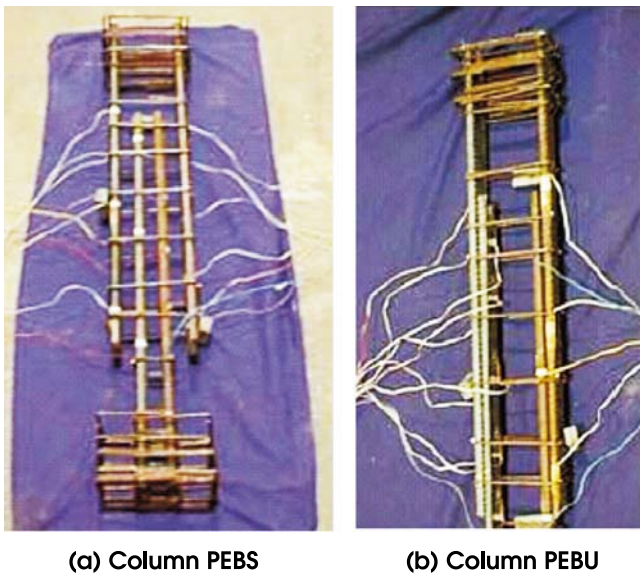
As shown in Figure 6, the symmetry axes of the jacks and of the plates were placed in line with the symmetry axes of the concrete section, to provide a centred load transmission to the column.
In the column tests, carried out with load control, two jacks and a load cell with a 1000 kN load capacity were used (Figure 6a).

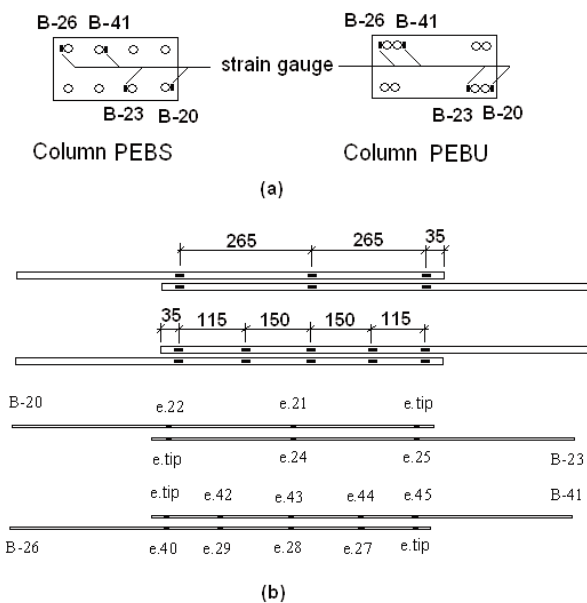**Figure 4 – Strain gauges position. (a): in the cross-section (b): in the splice (dimensions in mm)**
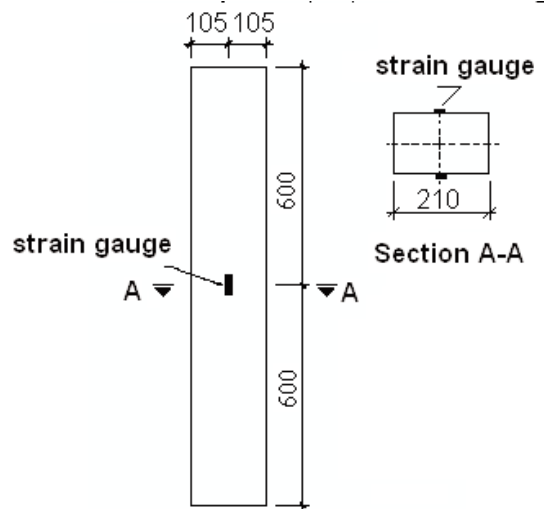

Figure 5 – Position of the strain gauges on the concrete (dimensions in mm)

The load was applied to the column at an approximate rate of 40 kN per minute, in three uninterrupted cycles: in the first one the column was loaded up to 400 kN and unloaded after that; in the second one the load reached 800 kN (approximately the service load of the element) and was again withdrawn; in the third one, the load was applied up to the column failure. Strains were continuously monitored during the test, up to the failure of the column.

3. Results

3.1 Failure Modes

The failure of both columns was sudden and occurred in a section at 300mm from the top of the column, in the region coinciding with the end of the splice, as shown in Figures 7 and 8.
Table 3 gives maximum load values (N_{max}) and the corresponding values of concrete strain (ε_c) at half the length of the column, and maximum strain ($\varepsilon_{s\ max.}$) of the compressed steel bars in the region of the failure (end of the splice) related to this load, obtained in the tests.
The smaller failure load of the PEBS column can be explained by the small distance between the longitudinal bars in the region where the failure occurred (see Figure 2, section 2.2), which reduced the contribution of these bars in the case of an eccentricity caused by imperfections.

3.2 Load-strain curves

Figure 9 shows typical load-strain of the longitudinal bars curves obtained in the tests. The curves shown in Figures 10 to 13 correspond to envelope curves for the load-strain curves in each load cycle.

Figure 6 – Details of the columns supports. (a): plate and steel support at the top and (b): plate at the bottom
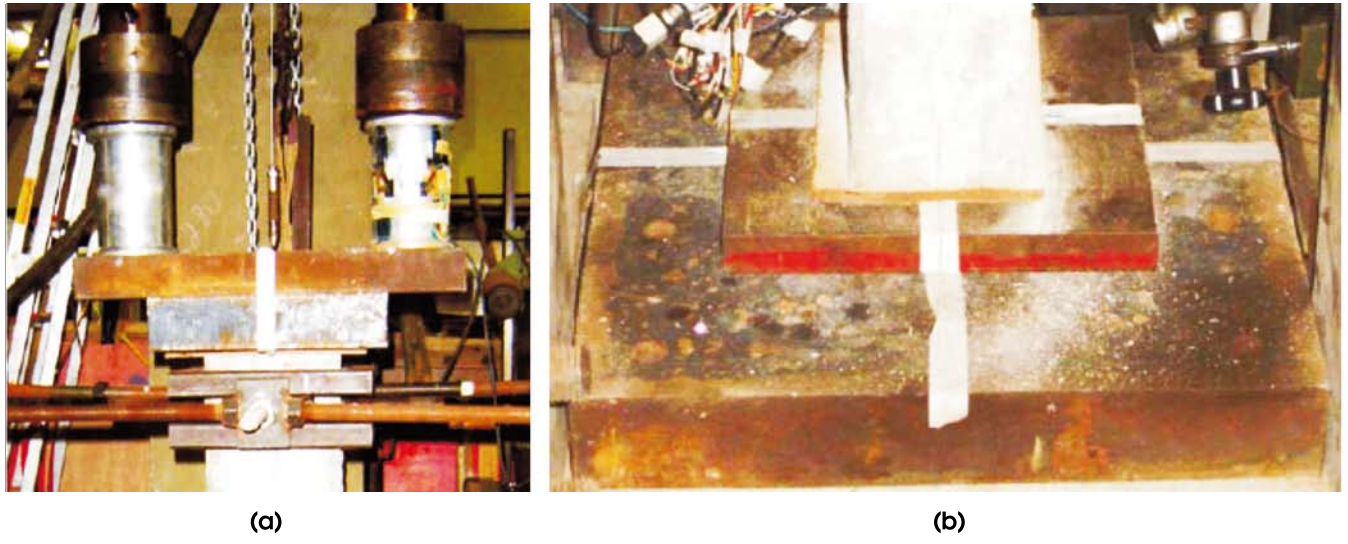
(a)

(b)

Figure 7 – Columns failure region

End of the splice

Figure 8 – Detail of the failure region
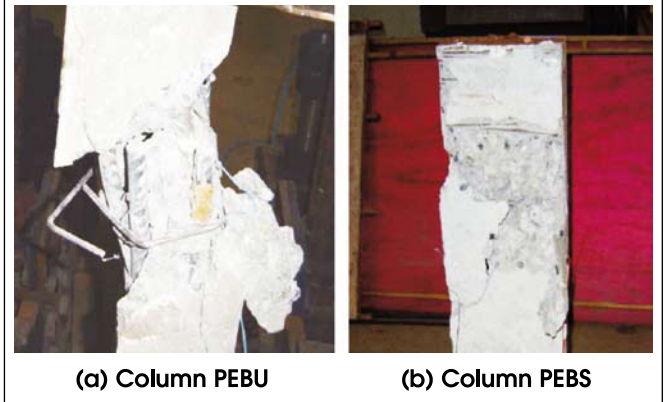
(a) Column PEBU   (b) Column PEBS

Figure 10 shows the load-concrete strain and Figure 11 the load-longitudinal bars strain for the PEBU column. The largest concrete strain and the largest strain in bars 26 and 41, on the same face of the PEBU column, show that the largest stresses occurred on this face of the column where the failure of the concrete took place.

For bars 26 and 41 (with five strain gauges) of both columns, the relationships between load and strains measured by the strain gauges that coincided in location with the strain gauges of bars 20 and 23 (with three strain gauges) were plotted, to allow the comparison of these strains.

Figure 12 shows the load-concrete strain curves and Figure 13 the load-longitudinal bars strain of the PEBS column. The largest concrete strain in the PEBS column, obtained from the strain gauge on the right face, and the largest strains obtained from the strain gauges located on bars 20 and 23, all on the same face

Table 3 – Test results

Column	$N_{máx.}$ (kN)	$\varepsilon_{c.}$ (‰)	$\varepsilon_{s\,máx.}$ (‰)
PEBU	1285	1.20	2.58
PEBS	985	1.30	2.10

**Figure 9 – Typical load-reinforcement strain curves.
(a): Bar 23 of column PBES and (b): Bar 23 of column PBEU**

(a)   (b)
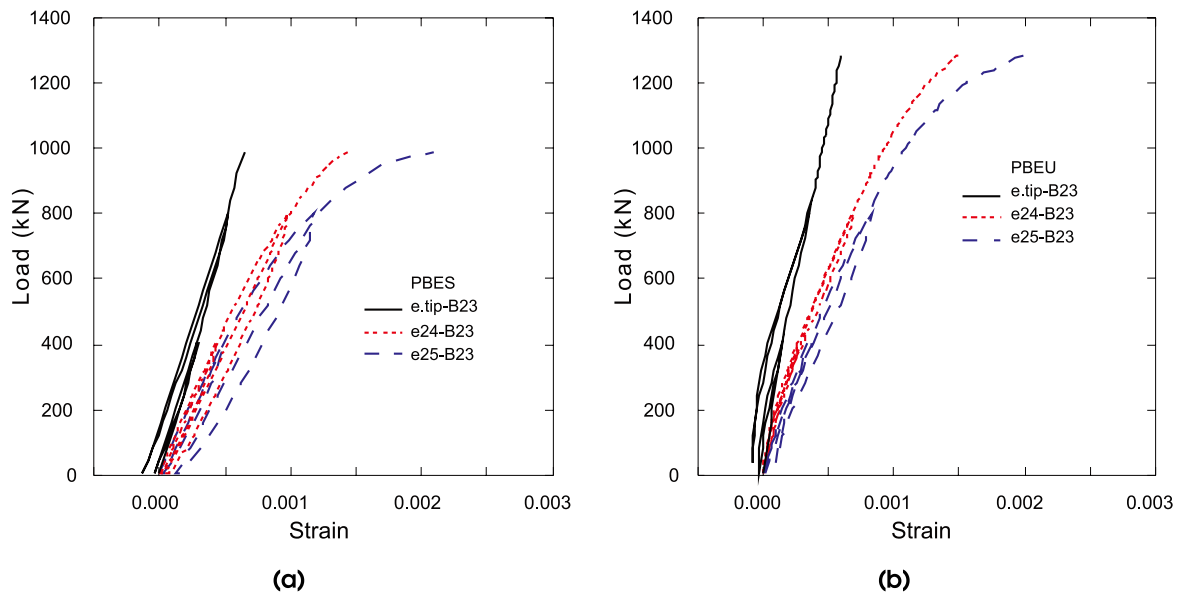
of the column, show that the highest stresses took place on this face, where the failure of the concrete occurred.

3.3 Longitudinal bars normal stress curves

The normal stresses of the longitudinal reinforcement bars were obtained from the measured strains and the stress-strain curve of the bars given in Figure 1.

Figures 14 and 15 show experimental values, joined by straight lines, of the normal stress along the splice of the longitudinal bars for the PEBU and PEBS columns, respectively, for the loads of 400 kN, 800 kN and for the failure load of each column.

Generally, for any load value, in both columns, the bar normal stress in the splice zone increased as the instrumented point moved away from the end of the bars, as shown in Figures 14 and 15. It is also possible to see in these two figures that the end of the bars displayed a smaller increase of the normal stress with the increase of the load, in comparison to the other points of the bars.

Figures 14 and 15 also show that the kind of variation of normal stress along the splices in both columns is similar. This gives evidence of the little influence of the spliced bars spacing on the global behaviour of a compression splice for the values of bars spacing adopted in this study.

3.4 Normal stress at the ends of the bars splice

In both columns, for the column failure load, the end of the bars displayed a normal stress value between 66 and 158MPa, as shown in Table 4, values being 2 to 5 times the uniaxial compressive strength of the concrete, f_c. Similar values were found by Pfister and Mattock (1963) and Scott et al. (1989) observed also that compression concrete stresses at the bars tips exceeded the uniaxial compressive strength of the concrete.

Table 4 shows the stresses in the bars at the ends of the splice: at the end of the bars (σ_p) and at the extremity of the splice opposite to it (σ_e), for loads of 400kN, 800kN and fail-

Figure 10 – Load-concrete strain envelope curves of column PEBU
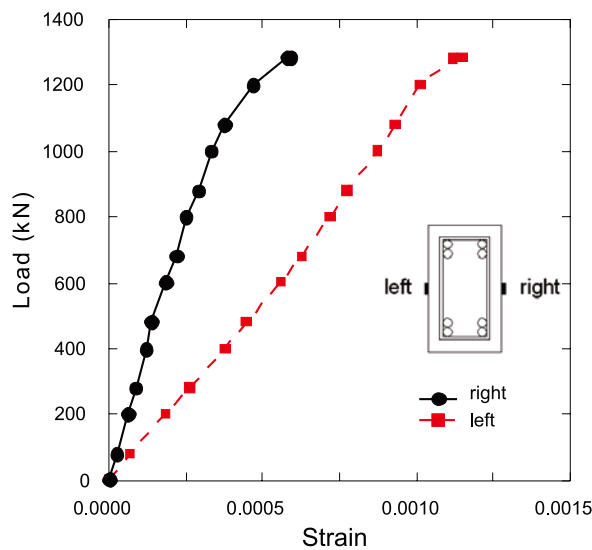
**Figure 11 – Load-reinforcement strain envelope curves.
(a): Bars 20 and 26 of column PEBU and (b): Bars 23 and 41 of column PEBU**

(a)

(b)
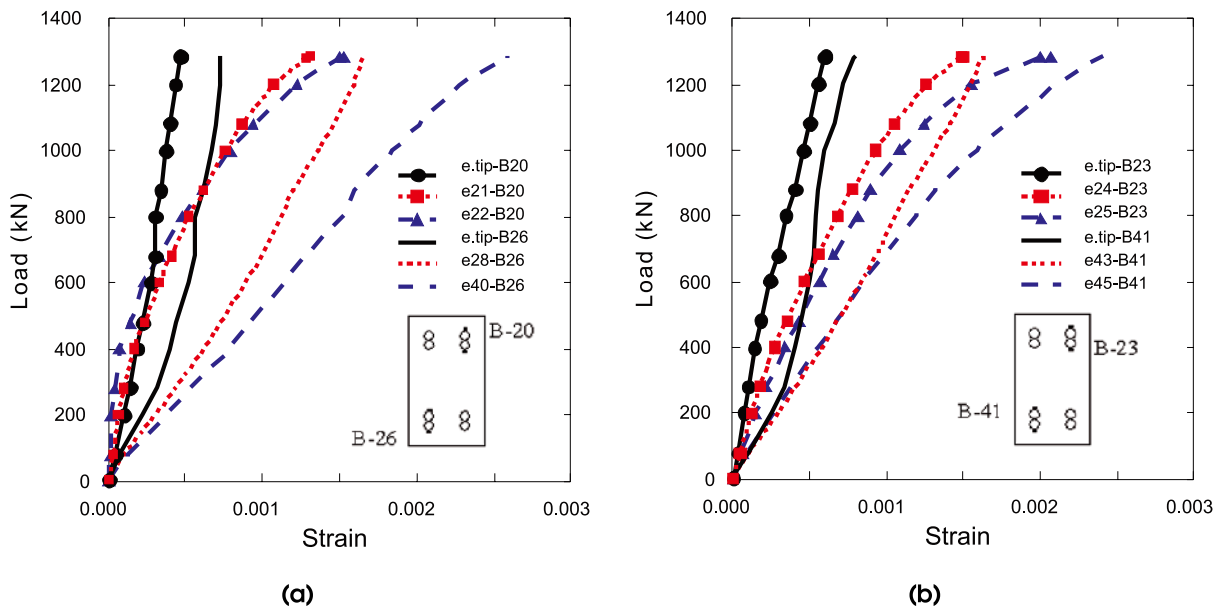
ure load. It is possible to see that, for all the bars, the σ_e/σ_p ratio increases with the increment of the load. For the failure load, σ_e/σ_p varies between 3 and 4.5.

3.5 Bond stress in the splice

Despite the fact that the load applied to both columns was centred, the distribution of the strains in a given cross-section was not uniform due to small imperfections. Consequently, for a same value of an applied load, the stresses in a particular bar (bar 41, for example) of both columns were different. To better compare the distribution of bond stresses along one same bar in both columns, the comparison is then made for a same strain value measured at the end of the splice opposite to the bar end.
Figure 16 shows the distribution of the bond stress (τ_i) in each region along the splice of bars 26 and 41, for strains of 0.0005, 0.0010 and 0.0013 at the end of the splice opposite to the bar end in both columns. In bars B-26 and B-41, from the normal

stresses in the five different positions where the strains were measured, the bond stresses were obtained in each one of the four regions between these five positions, through the expression

$$\tau_i = \frac{\pi\phi^2}{4u}\frac{\Delta\sigma_s}{\Delta x}$$

where u is the contact perimeter between the bar and the concrete along the length Δx between two consecutive positions, $\Delta\sigma_s = \Delta\varepsilon_s E_s$, $\Delta\varepsilon_s$ is the difference between the strains measured in these two positions and E_s is the steel modulus of elasticity (210000 MPa). The same procedure was adopted for bars B-20 and B-23, but with the number of regions equal to two, as there were only three strain gauges on them.
Table 5 shows the values for mean bond stress τ_m related to the entire length of the splice, obtained with the expression

$$\tau_m = \frac{1}{n}\sum_{i=1}^{n}\tau_i$$

where n = 2 for bars B-20 and B-23 and n = 4 for bars B-26 and B-41.

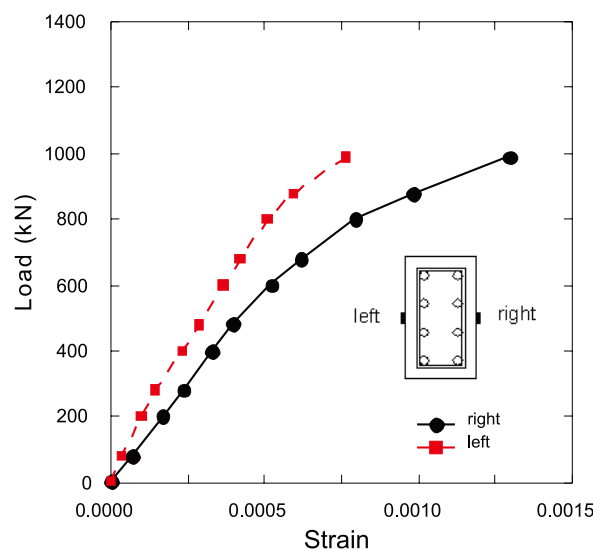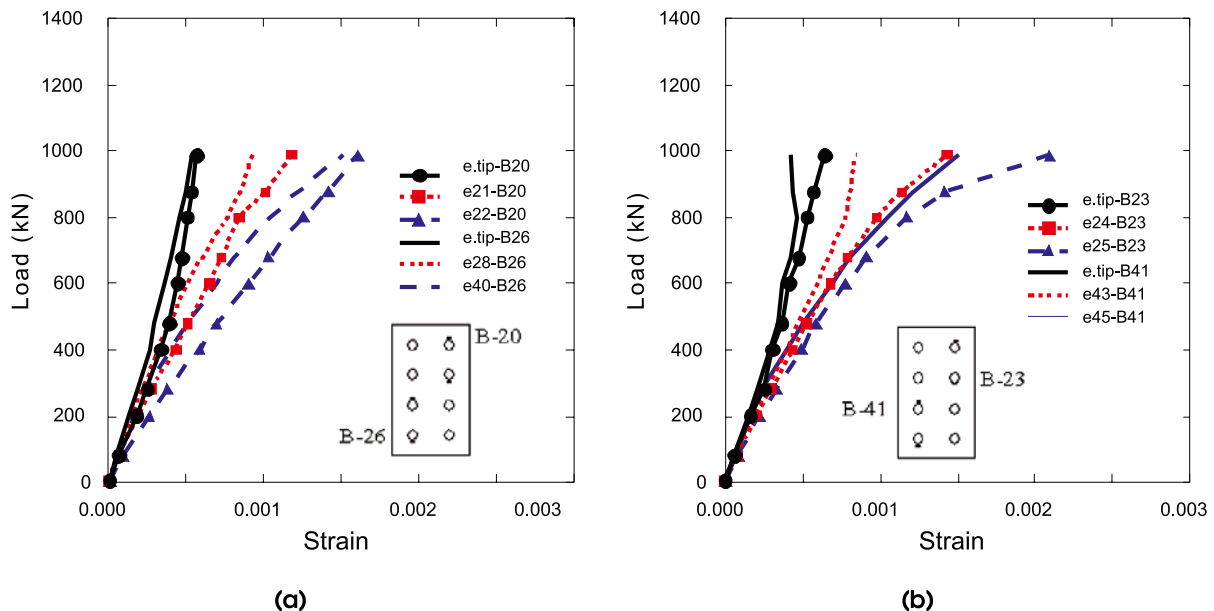**Figure 12 – Load-concrete strain envelope curves of column PEBS**

Figure 13 – Load-reinforcement strain envelope curves.
(a): Bars 20 and 26 of column PEBS and (b): Bars 23 and 41 of column PEBS

In figure 16, the values of τ_i are higher at the splice ends and the stress near the bar end tends to be higher. Scott et al. (1989), when testing elements with compression spliced bars, noted that the highest values of bond stress occurred at the tips of the bars. In her turn, Quintana (2005), in 12 columns with spliced bars submitted to eccentric compression, noted that generally the highest values of τ_i occurred in the regions nearest to the tip of the bars.

As shows Table 5, the mean bond stresses in both columns, corresponding to the strains of 0.0010 and 0.0013 at the end of the splice opposite to the bar tip, do not present differences higher than around 20%. Taking into account the possible imperfections of the columns, one can say that the global behaviour of the splice in the two columns was similar. Tests of beams with tension bars in contact or with spacing equal to ϕ_l and $2\phi_l$ (CHAMBERLIN, 1958) or to $2.5\phi_l$ (CHINN, FERGUSON and THOMPSON, 1955) in the splices showed also no relevant difference between the strengths of these splices. These results show that, in spite of the lack of concrete fully involving the contact bars in the splice, with the transverse reinforcement used, this splice was capable of developing bond stress of the same order as the splice with $2\phi_l$ bars spacing. According to Walker (1951), an adequate concrete vibration during casting can guarantee a good penetration of the mortar between the ribs of the contact bars and a good bond between the bars and the mortar, and there is no evidence that the mortar between these bars is of lower quality in relation to the concrete around the separated bars.

For the failure load, the values of τ_m in the two columns were around 2MPa.

4. Conclusions

This work made an experimental analysis of two columns subjected to centred compression, both with lapped splices: one with the bars in contact and another with the bars spacing equal to twice the diameter of the bars. The results showed that:

- For both columns, at failure load, the tips of the bars had a normal stress value from 2 to 5 times the compressive strength of the concrete. For all the bars, the ratio between the normal stresses at the ends of the splice (σ_e/σ_p) increased with the increase of the load.
- The values of bond stress (τ_i) in both columns were higher at the ends of the splices, and the stress near the tip of the bars tended to be higher.
- The mean bond stresses in the splices of both columns were similar. This shows the little influence of bars spacing on the global behaviour of the compression splice.

It is advisable to extend this study to a larger number of tests of columns with lap compression splices where the spacing between the bars covers a greater range of values.

5. Acknowledgements

6. References

[01] CHAMBERLIN, S.J. Spacing of spliced bars in tension pull-out specimens. ACI Journal Proceedings, vol. 49, No. 4, part 1. Dec. 1952.

[02] CHAMBERLIN, S. J. Spacing of spliced bars in beams. ACI Journal, Proceedings, vol. 54, No. 8, p.689-691, Feb. 1958.

[03] CHINN, J., FERGUSON, P. and THOMPSON, J. Lapped splices in reinforced concrete beams. ACI Journal Proceedings, vol. 52, No. 2, Oct. 1955.

[04] HAMAD, B.S. and MANSOUR, M. Bond strength of noncontact tension lap splices. ACI Structural Journal, vol.93, No. 3, p. 316-326, May-June 1996.

[05] PFISTER J.F. and MATTOCK A.H. High strength bars as concrete reinforcement. Part 5. Lapped splices in concentrically loaded columns. Journal of the PCA. Research and Development Laboratories. p.27-40. May 1963.
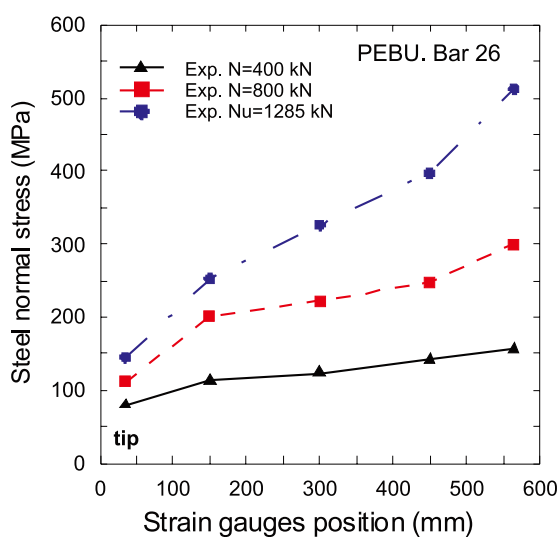
**Figure 14 – Normal stress distribution along the lap of column PEBU.
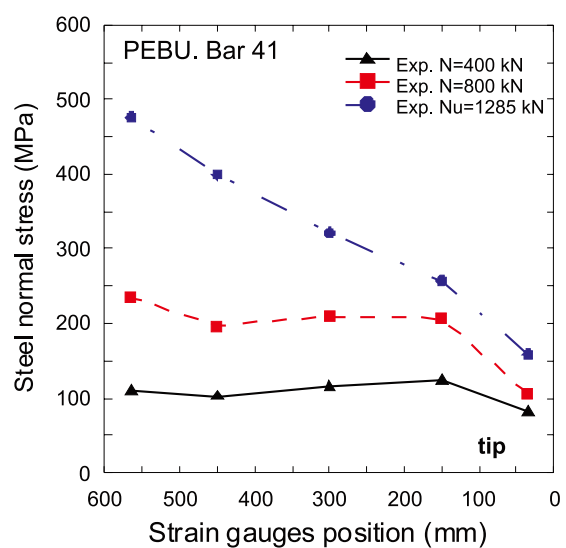(a): bar 20; (b): bar 23; (c): bar 26; (d): bar 41**
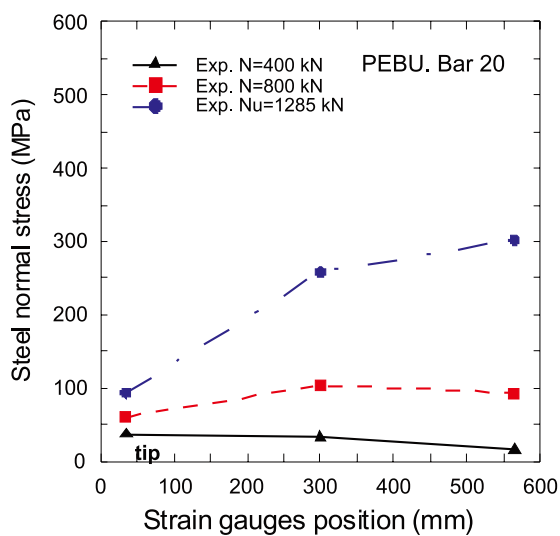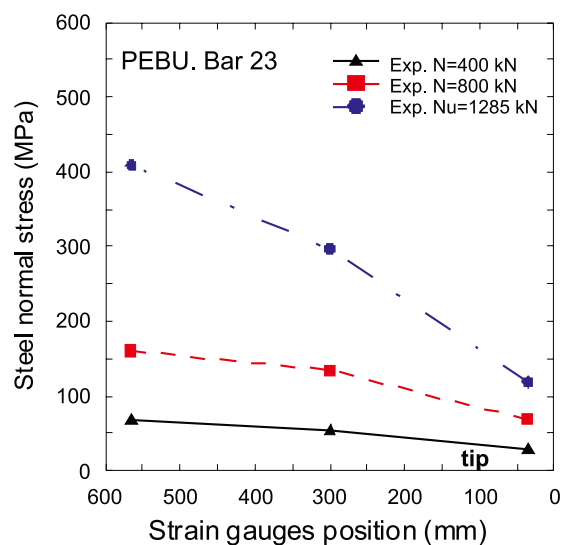
[06]   QUINTANA, C.B. Influência da Armadura Transversal
       e do Cobrimento da Armadura Longitudinal na
       Resistência de Pilares de Concreto. Tese de
       Doutorado, Departamento de Engenharia Civil,
   PUC-Rio, 174p. Rio de Janeiro, Setembro, 2005.

[07]   SCOTT, R.H., GILL, P.A.T and JUDGE, R.C.B.
       Force transfer in compression lap joints in reinforced
       concrete. Magazine of Concrete Research, vol.41,
       No. 146, March 1989.

[08]   WALKER, W.T. Laboratory tests of spaced and tied
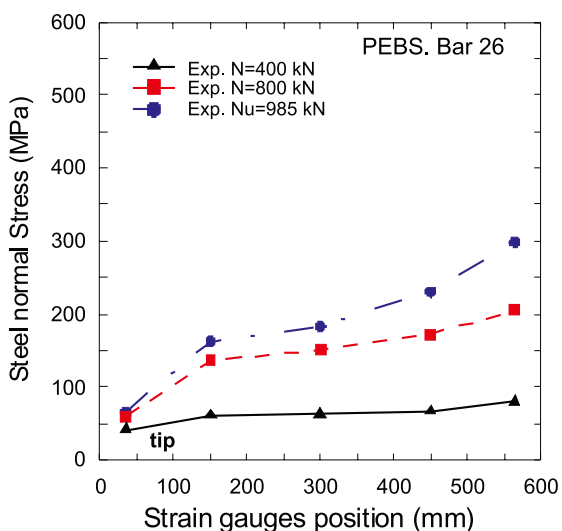   reinforcing bars. ACI Journal Proceedings, vol. 47,
       No. 5, p.365-378, Jan. 1951.

**Figure 15 – Normal stress distribution along the lap of column PEBS.
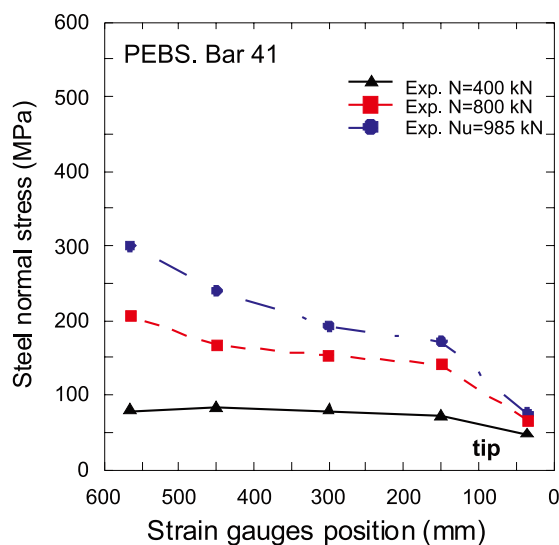(a): bar 20; (b): bar 23; (c): bar 26; (d): bar 41**
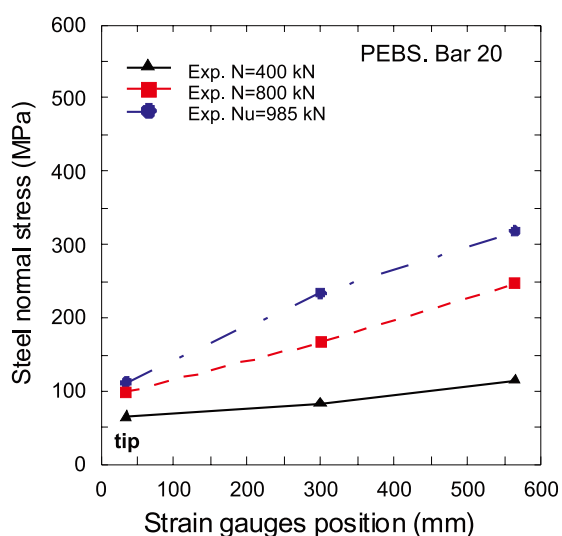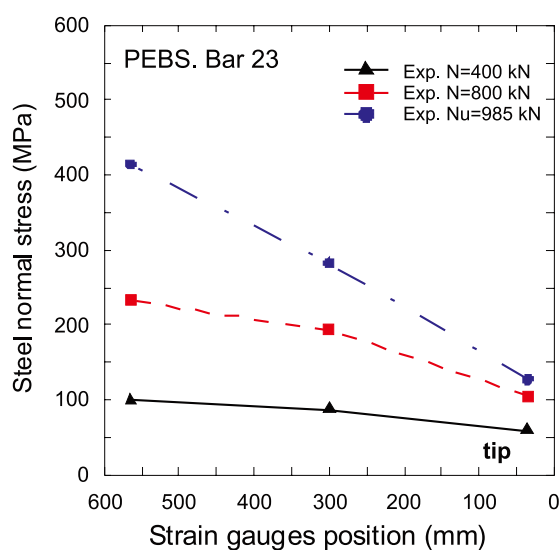
Table 4 – Normal stress at the ends of the splices (Load: kN; stress: MPa)

Column		PEBU				PBES		
Bar	Stress	Load				Load		
		400	800	1285		400	800	985
C20	σ_p	37,4	61,0	93,6		65,2	98,9	112,1
	σ_e	15,2	93,6	302,1		114,7	247,2	318,4
	σ_e / σ_p	**0,4**	**1,5**	**3,2**		**1,8**	**2,5**	**2,8**
C23	σ_p	27,6	67,9	118,6		59,3	104,4	127,2
	σ_e	67,3	160,4	408,7		98,9	231,7	414,0
	σ_e / σ_p	**2,4**	**2,4**	**3,4**		**1,7**	**2,2**	**3,3**
C26	σ_p	79,6	111,1	144,8		41,4	60,0	65,7
	σ_e	155,3	299,4	511,8		79,1	205,7	298,7
	σ_e / σ_p	**2,0**	**2,7**	**3,5**		**1,9**	**3,4**	**4,5**
C41	σ_p	80,7	106,8	158,2		47,0	66,0	75,2
	σ_e	109,6	235,0	475,7		79,1	205,7	298,7
	σ_e / σ_p	**1,4**	**2,2**	**3,0**		**1,7**	**3,1**	**3,9**

Table 5 – Mean bond stress

τ_m (MPa)				
Column	Bar	Strain		
		0.0005	0.0010	0.0013
PEBU	B-20	0.70	0.94	1.34
	B-23	0.47	0.92	1.29
	B-26	0.36	0.98	1.22
	B-41	0.60	1.27	1.56
PEBS	B-20	0.30	1.12	1.26
	B-23	0.37	0.89	1.20
	B-26	0.41	0.99	1.39
	B-41	0.36	0.99	1.46

Figure 16 – Bond stress distribution along the splice of bars B-26 and B-41 of columns PEBU and PEBS